# 18

# Use of a-SiC:H Photodiodes in Optical Communications Applications

P. Louro[1,2], M. Vieira[1,2,3], M. A. Vieira[1,2],
M. Fernandes[1,2] and J. Costa[1,2]
[1]*Electronics Telecommunications and Computer Dept, ISEL, Lisbon*
[2]*CTS-UNINOVA, Lisbon*
[3]*DEE-FCT-UNL, Quinta da Torre, Monte da Caparica, 2829-516, Caparica*
*Portugal*

## 1. Introduction

### 1.1 Short range optical communications

Silica single mode optical fiber is widely used in long distance communication systems for high speed data transmission (Gbit/s) because of its high bandwidth and low attenuation coefficient. The use of this fiber for short-distance interconnection is not preferred due to the small core diameter of the single-mode fiber, and consequently high requirements for coupling and adjustments. Therefore, in local systems it is preferable to use multi-mode fiber which has greater diameter. The plastic optical fiber (POF) is a suitable, promising solution as transmission medium for short range communications [M. Kagami 2007, M. Kuzyk 2008, O. Zieeman et al 2007]. Its core diameter (250-1000 μm) offers the possibility to use inexpensive polymer connectors and its flexibility enables bending radii, which are by far more critical for glass fibers. Besides, it is more resilient to damage than glass due to its intrinsic material characteristics. It is easier to terminate, polish, and connect as well, which can reduce the cost of installation and maintenance.

There are many uses for POF. A few possibilities include short range networking, e.g. indoor and LAN applications, which are directly related to the simplicity of connection and use and therefore to a significant reduction in installation costs. Another sector where POF displaces the traditional communication medium is in-house communication networks (light switches, door bell, temperature measurement, smoke detection, moisture measurement, counters) [W. Stallings 2007], although the possibilities of application are not confined inside of the house itself. Today, Internet technologies are used to transmit more and more images and develop new services that require more data (high definition TV, movies on demand communications videos that may lead to applications such as tele-assistance of persons alone, sick and elderly,...). The use of the data transmission technology DSL pair Telephone wire is no longer sufficient to meet these new demands. This fiber added at the user provides a data transmission speed Internet 10 times greater than current supply. Note that the approach of wiring the building using fiber Adds value to the appartmenmts and allows residents to enjoy the services supplied by the fiber. In the future POF will most likely displace copper cables for the so-called last mile between the last

distribution box of the telecommunication company and the end-consumer. Today, copper cables are the most significant bottleneck for high-speed internet "Triple Play", the combination of VoIP, IPTV and the classical internet, is introduced in the market forcefully and therefore high-speed connections are essential. It is highly expensive to realize any VDSL system using copper components, thus the future will be FTTH. POF can be applied in the house itself for different scenarios, such as "A/V Server Network" (communication between e.g. television, hi-fi-receiver and DVD-player), "Control Server Network" (messaging between e.g. refrigerator and stove) or "Data Server Network" (data exchange between e.g. notebook and printer).
Another field of recent application is the auto industry, where the main benefits from POF arise from the tight bending radius that makes POF well-suited to the automobile environment. The installation of multiple networks in modern cars, and the expansion of these systems have quickly accelerated. Sensors, in a car network (electric windows, electric mirrors, locks and even power-seat controls on the door) can be planned to be coupled over wireless interfaces with other active devices (such as lights, shutters, local and remote displays, alarms).
Other possible industrial sectors include consumer electronics, the aerospace industry, due to the lighter weight, or the medical sector, namely medical imaging for image-transfer applications. But all these applications have one thing in common – they all need high-speed data transmission capabilities. To increase bandwidth for this technology the only possibility is to increase the data rate, which lowers the signal-to-noise ratio and therefore can only be improved in small limitations.

### 1.2 Wavelength division multiplexing technique

The explosion in demand for network bandwidth is largely due to the growth in data traffic. Leading service providers report bandwidths doubling on their backbones about every six to nine months. This is largely in response to the 300 percent growth per year in Internet traffic, while traditional voice traffic grows at a compound annual rate of only about 13 percent [D. Nolan et al 2002]. At the same time that network traffic volume is increasing, the nature of the traffic itself is becoming more complex.
Faced with the challenge of dramatically increasing capacity while constraining costs, carriers have two options: Install new fiber or increase the effective bandwidth of existing fiber. Laying new fiber is the traditional means used by carriers to expand their networks. Deploying new fiber, however, is a costly proposition. Laying new fiber makes sense only when it is desirable to expand the embedded base.
Increasing the effective capacity of existing fiber can be accomplished in two ways, which include the increase of the bit rate in the existing systems or the increase on the number of wavelengths transmitted by the fiber. This latter option to enlarge the transmission capacity of the waveguide is designated the Wavelength-Division-Multiplexing (WDM) techniques, which in glass fiber technology within the infrared range has long been an established practice.
The standard communication over POF uses only one single channel [W. Daum et al 2002]. To increase the bandwidth, and consequently the data transmission speed, the only possibility is to increase the data rate, which lowers the signal-to-noise ratio and therefore offers limited improvements. One approach for increasing the capacity of the waveguide is to use WDM techniques. In glass fiber technology, the use of WDM in the infrared range has

long been an established practice. This multiplexing technology uses multiple wavelengths to carry information over a single fiber.
For WDM two key-elements are indispensable, a multiplexer (MUX) and a demultiplexer (DEMUX). The multiplexer takes optical wavelengths from multiple fibers and makes them converge into one beam. At the receiving end the system must be able to separate out the components of the light so that they can be detected. Demultiplexers perform this function by separating the received beam into its wavelength components and coupling them to individual fibers (Fig. 1).


Fig. 1. Multiplexing and Demultiplexing operations.

The standard MUX/DEMUX devices are well known for infrared telecom systems [M. Bas 2002]. These devices can be either passive or active in design. Passive designs are based on interference filters and plane diffraction gratings, while active designs combine passive devices with tunable filters. Most of these devices require additional collimating and focusing optics that need alignment and lead to complicated designs. Figure 2 shows the sketch of the basic concept of a DEMUX device for optical communication where the different wavelengths are separated using a prism.

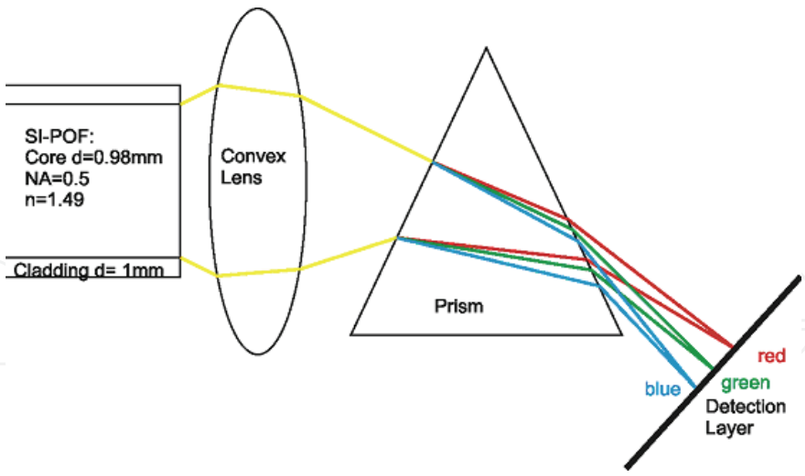


Fig. 2. Demultiplexer device based on an optical component.

The primary challenges of these devices are to minimize cross-talk and maximize channel separation. Cross-talk is a measure of how well the channels are separated, while channel separation refers to the ability to distinguish each wavelength. Between multiplexing and demultiplexing points in a DWDM system, there is an area in which multiple wavelengths exist. It is often desirable to be able to remove or insert one or more wavelengths at some point along this span. An optical add/drop multiplexer (OADM) performs this function.

Rather than combining or separating all wavelengths, the OADM can remove some while passing others on. OADMs are a key part of moving toward the goal of all-optical networks. Usually, demultiplexing must be done before the light is detected, because standard photodetectors (based on crystalline materials) are inherently broadband devices that cannot selectively detect a single wavelength.
This basic concept of the use of WDM can also be assigned to POF. However POF shows a different attenuation behavior, with better performance in the visible window of the spectrum. For this reason, only the visible spectrum can be applied when using POF for communication. This limitation demands the design of new devices for the implementation of this technique using POF technology [S. Randel et al 2007, M. Haupt 2006]. Several technical solutions for this problem are available, but none of them can be efficiently utilized in the POF application scenario described here, mostly because these solutions are all afflicted with high costs and therefore not applicable for mass production. A solution to overcome the bandwidth bottleneck of standard POF communication is to adapt WDM for the visible wavelength range. Therefore newly designed multiplexers and demultiplexers are essential.

## 2. WDM based on amorphous technology

### 2.1 WDM over POF

The use of multilayered structures based on a-SiC:H alloys as photo-sensing or wavelength sensitive devices in the visible range, has been widely studied in the past for different applications, namely, solar cells, color sensors, optical sensors [G. Cesare et al 1995, A. Zhu at al 1998, M. Topic et al 2000, M. Mulato et al 2001]. In these multilayered devices the light filtering is achieved through the use of different band gap materials, namely a-$Si_{1-x}C_x$:H. In these devices the spectral sensitivity in the visible range is controlled by the external applied voltage. Thus, proper tuning of the device sensitivity along the visible spectrum allows the recognition of the absorbed light wavelength [H. Tsai 1987, H. Stiebig et al 1995]. Using this operation principle, other applications were developed, such as, the optical image sensor LSP (Laser Scanned Photodiode) reported by M. Vieira et al 2002, the CLSP (Color Laser Scanned Photodiode) by P. Louro et al 2007 and M. Vieira et al 2008 or the currently under development optical WDM device [P. Louro et al 2009, M. Vieira et al 2010].
In this chapter the wavelength sensitive transducers are optimized to take advantage of the whole visible spectrum. The challenges in this development are mainly related to the ability of the transducer to discriminate wavelengths, which is directly related to the bandwidth of the communication system. Other technical issues related to the signal attenuation and to the light-to-dark sensitivity of the optical device will also be analysed.
Those transducers present several advantages as they:

- are active optical transmission devices and receive-side opto-electronic devices that convert light pulses into electrical signals.
- amplify all the wavelengths at once and can be also used to boost signal power.
- can be active designs combining passive devices with tunable filters and are able to remove or insert one or more wavelengths at some point. An optical add/drop multiplexer (OADM) performs this function.
- combine several lower-bandwidth streams of data into a single beam of light and they are therefore required to be wavelength selective, allowing for the transmission, recovery, or routing of specific wavelengths, where the device behaves like a wavelength converter.

### 2.2 Device configuration and operation

#### 2.2.1 Configuration

The WDM device is a double heterostructure (Fig. 3b) produced by PECVD (Plasma Enhanced Chemical Vapor Deposition). Deposition conditions are described elsewhere [M. Vieira et al 2007]. The thickness and the absorption coefficient of the front photodiode are optimized for blue collection and red transmittance, and the thickness of the back one adjusted to achieve full absorption in the greenish region and high collection in the red spectral one. As a result, both front and back diodes act as optical filters confining, respectively, the blue and the red optical carriers, while the green ones are absorbed across both [Louro et al 2007]. In Fig. 3a it is displayed the recombination profiles (straight lines) under red ($\lambda_R$ =650 nm) green ($\lambda_G$ =550 nm) and blue ($\lambda_B$ =450 nm) optical bias and different electrical bias (-6V<V<0V). The generation profiles are also shown (symbols). We used a device simulation program ASCA-2D [A. Fantoni et al 1999] to analyze the profiles in the investigated structures.

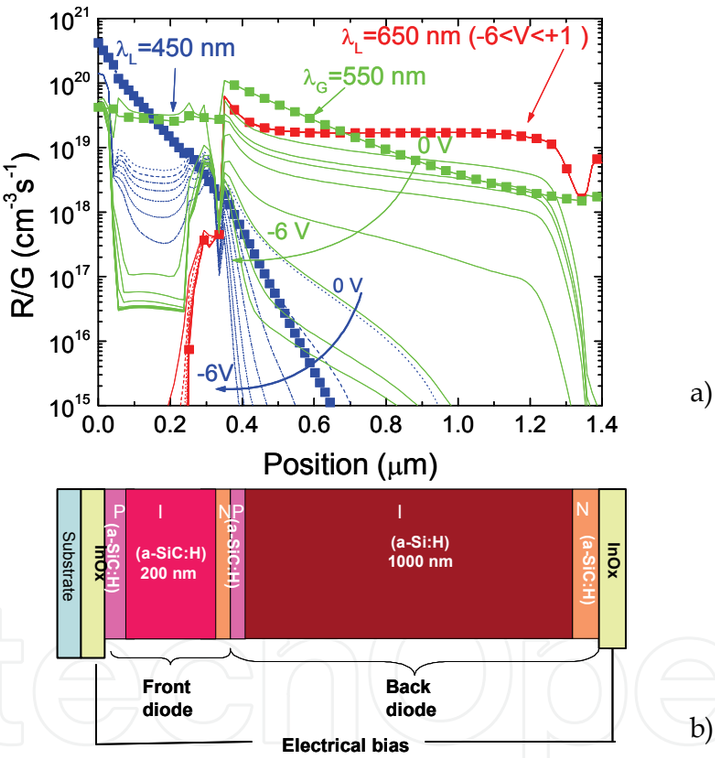


Fig. 3. a-SiC:H WDM device. a) Recombination profiles (straight lines) under red ($\lambda_R$ =650 nm) green ($\lambda_G$ =550 nm) and blue ($\lambda_B$ =450 nm) optical bias and different applied voltages (-6V<V<0V). The generation profiles are also shown (symbols). b) Device configuration.

The WDM device consists of a glass/ITO/a-SiC:H (p-i-n) photodiode which faces the incoming modulated light followed by an a-SiC:H(-p) /Si:H(-i')/SiC:H (-n')/ITO heterostructure that allows the optical readout. By reading out, under different applied bias, the total photocurrent generated by all the incoming optical carriers the information (wavelength, modulation frequency) is multiplexed or demultiplexed and can be transmitted or recovered again [M. Vieira et al 2008].

### 2.2.2 WDM working principle

In Figures 4 the device configuration is depicted in both multiplexing and demultiplexing modes. Here, multiple monochromatic (Figure 20) or a single polychromatic (Figure 21) beams are directed to the device where they are absorbed, accordingly to each wavelength, giving rise to a time and wavelength dependent electrical field modulation across it [M. Vieira et al 2001].

In the multiplexing mode the device faces the modulated light incoming together from the fibers, each with a wavelength in a specific range (R, G, B channels). The combined effect of each input channel is then converted to an electrical signal via the WDM device (Figure 19a) keeping the memory of the input channels (wavelength and bite rate).

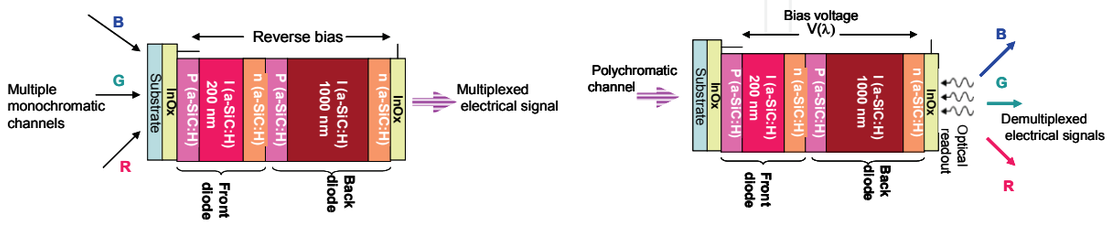


a) b)

Fig. 4. WDM device configuration : a) multiplexing mode, b) demultiplexing mode.

In the demultiplexing mode a polychromatic light beam (mixture of different wavelength) is projected onto the device and the signal measured at appropriate applied voltages. Here, the spectral sensibility of the device is voltage controlled allowing the recognition of the RGB channels (Figure 4b).

### 2.3 Optical characterization

### 2.3.1 Spectral response

The devices were characterized through spectral response measurements (400-800 nm), under different modulated light frequencies (15 Hz to 2 KHz) and electrical bias (-10V to +3V). In Figure 5a it is displayed, under reverse bias, the spectral photocurrent at different frequencies and, in Figure 5b, the trend with the applied voltages is shown at 2 KHz.

Different trends with the frequency are observed. Under reverse bias and low frequencies (f<400Hz), the spectral response increases with the frequency in the reddish region while in the blue/green spectral regions the photocurrent remains constant (Figure 5a). For higher frequencies (f>400Hz) the spectral response does not depend on the modulated light frequency and, as the applied voltage changes from forward to reverse (Figure 5b), the blue/green spectral collection is enlarged while the red one remains constant.

### 2.3.2 Voltage controlled sensitivity

In Figure 6a it is displayed the measured spectral photocurrent and in Figure 6b the ac current-voltage characteristics under illumination are shown. In this last measurement three modulated monochromatic lights: R ($\lambda_R$=626 nm); G ($\lambda_G$=520 nm) and B ($\lambda_B$=470 nm), and their polychromatic combinations; R&G (Yellow); R&B (Magenta); G&B (Cyan) and R&G&B (White) illuminated separately the device and the photocurrent was measured as a function of the applied voltage. As light sources ultra-bright LEDs were used with a 20 nm spectral bandwidth. The output optical power was adjusted for each independent wavelength at 19 $\mu W/cm^2$.

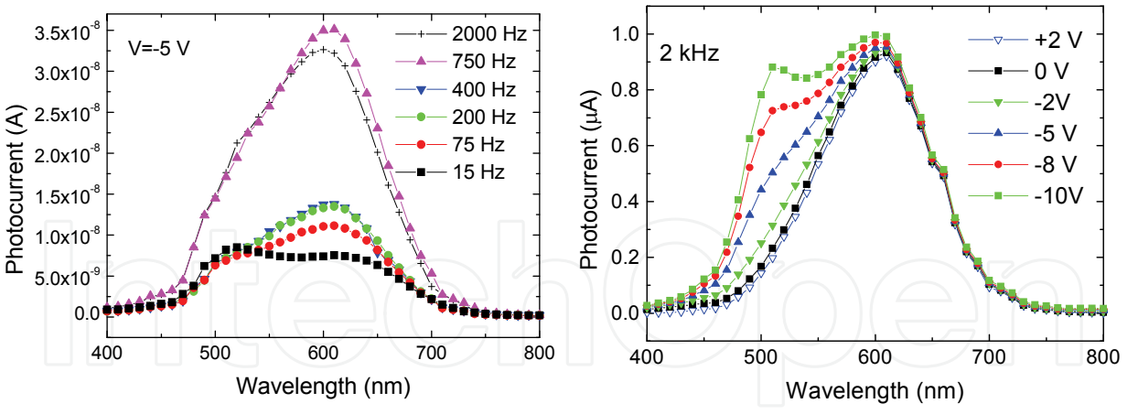


a) b)

Fig. 5. Spectral photocurrent under: a) reverse bias (-5V) and different frequencies; b) different applied voltages and at a modulated frequency of 2000 Hz.

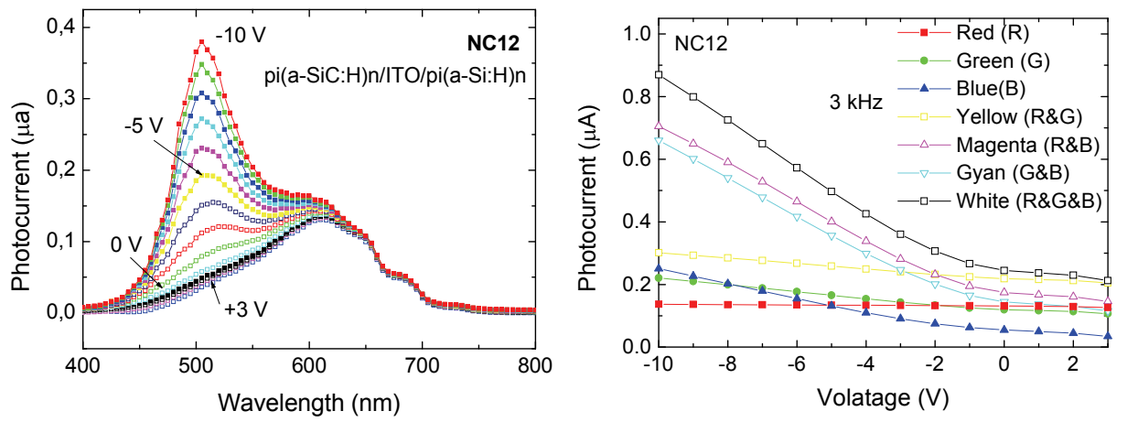


a) b)

Fig. 6. a) Spectral response at different applied bias. b) Photocurrent voltage characteristics under different light wavelengths.

Data from Figure 6 confirm that, as the applied voltage changes from forward to reverse the blue/green spectral collection is enlarged while the red one remains constant (Figure 6a). The photocurrent under red modulated light (Figure 6b) is independent on the applied voltage while under blue, green or combined irradiations; it increases with the reverse bias. If the blue spectral component is present (B&R, B&G), a sharp increase with the reverse bias is observed. Under positive bias the blue signal becomes negligible and the R&B, the G&B and the R&G&B multiplexed signals overlap, respectively with the R, the G and the R&G signals. This behavior illustrates, under forward bias, the low sensitivity to the blue component of the multiplexed signal. It is interesting to notice that under reverse bias the green signal has a blue-like behavior, while under forward bias its behavior is red-like confirming the green photons absorption across both front and back diodes.
In Figure 7 (a, c) the spectral photocurrent under different electrical bias and its trend (b, d) with the applied voltage, under specific wavelengths, are displayed separately for the front, p-i' (a-SiC:H)-n, and back p-i (a-Si:H)-n, photodiodes. Here, the internal transparent ITO contact was used to apply the voltage (Figure 4).

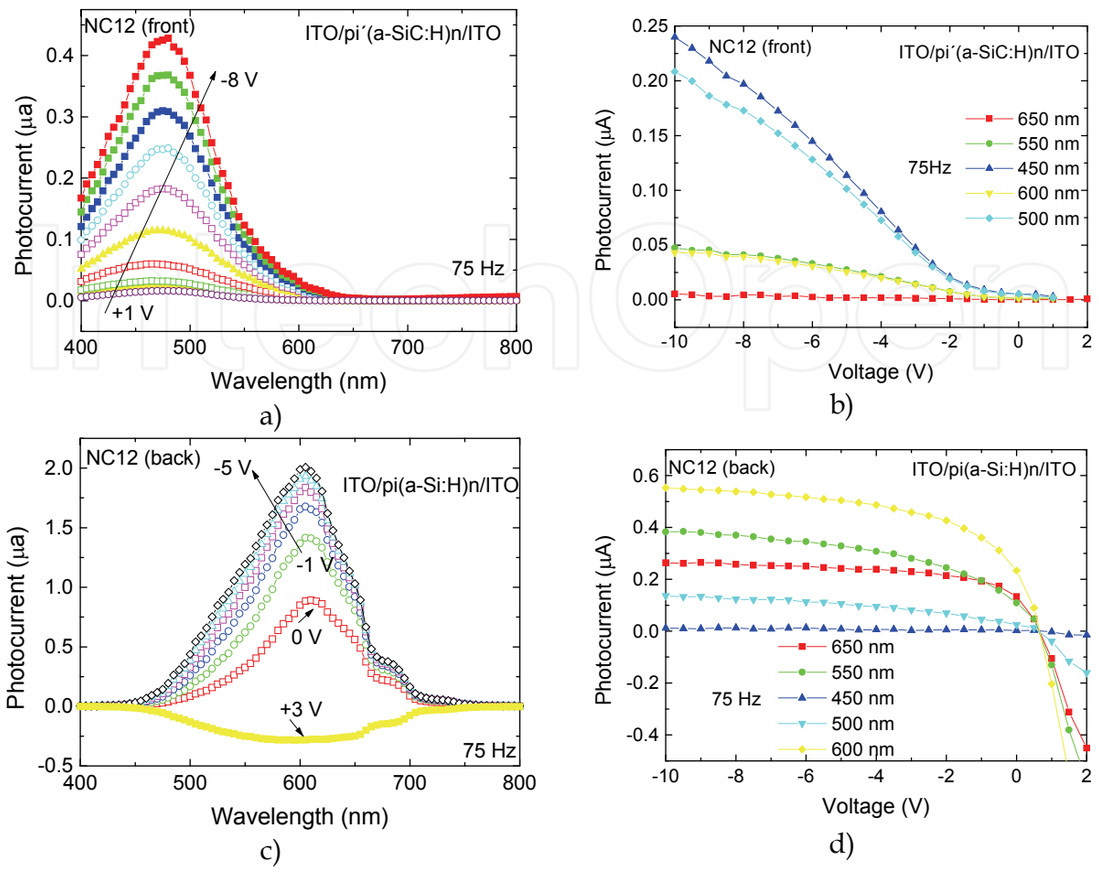


Fig. 7. Spectral photocurrent under different applied bias (a, c) and its trend with the applied voltage, at different wavelengths (b, d), for the front, p-i' (a-SiC:H)-n, and back, p-i (a-Si:H)-n.

Results confirm that the front and back photodiodes act as optical filters, respectively in the blue and red spectral regions. The front diode, based on a-SiC:H, cuts the red component of the spectrum while the back one, based on a-Si:H, cuts the blue component. Each diode separately presents the typical responses of single p-i-n structures while the stacked configuration (Figure 6a) shows the influence of both front and back diodes modulated by its interconnection through the internal n-p junction.

### 2.3.3 Selective wavelength discrimination

In Figure 8 it is displayed, the spectral photocurrent under negative (-10V) and positive (+3V) external bias and its differences (symbol), the dot lines show the multi peak curve fit at -10V.

Under negative bias the contribution of both front and back diodes (dotted lines) is clear. Two peaks centered, respectively at 500 nm and 600 nm are observed. Under positive bias, the response around 500 nm disappears while the one around 600 nm remains constant as expected from Figure 6a. So, under forward bias the device becomes sensitive to the red region and under reverse bias to the blue one working as a selective optical device in the visible range.

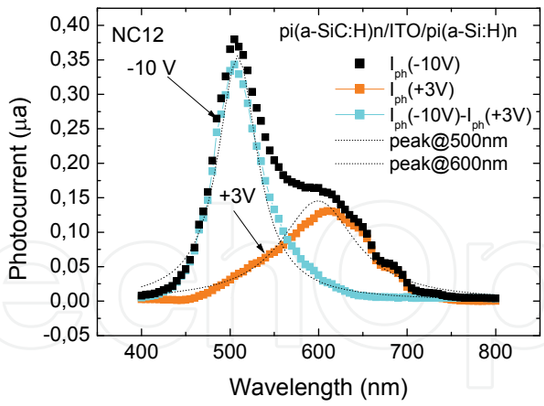


Fig. 8. Spectral response at under negative and positive electrical bias.

### 2.3.4 Frequency dependence

In Figure 9 the ac current-voltage characteristics under different wavelengths: 650 nm (R); 450 nm (B); 650 nm & 450 nm (R&B), and at the low and high frequency regimes is displayed.

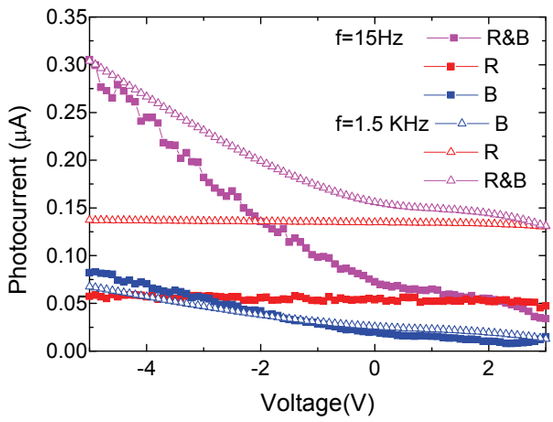


Fig. 9. ac IV characteristics under R (λL =650 nm); B(L =450 nm), R(L =650 nm) & B L =450 nm) modulated light and different light frequencies (15Hz;1.5KHz).

Results show that in both regimes, under red modulated light, the collection efficiency remains always independent on the applied voltage being higher at high frequencies, as expected from Figure 6a. Under blue irradiation the collection does not depend on the frequency regime. Those effects suggest different capacitive effects in both front and back diodes.

## 3. Wavelength division multiplexing device

### 3.1 Voltage controlled device

The effect of the applied voltage on the output transient multiplexed signal is analyzed. To readout the combined spectra, the generated transient photocurrent due to the simultaneous effect of two ($\lambda_R$ =650 nm, $\lambda_B$ =450 nm) and three ($\lambda_R$ =650 nm, $\lambda_G$ =550 nm, $\lambda_B$ =450 nm) pulsed monochromatic channels was measured, under different applied voltages (Fig. 10).

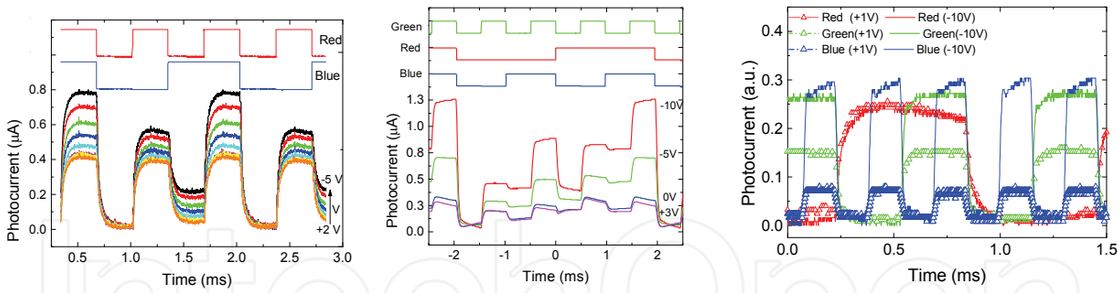


a) b) c)

Fig. 10. Transient multiplexed signals at different applied voltages and input wavelengths: a) R&B (λR,B=650nm, 450 nm). The highest frequency of the input signal is 1.5 kHz. b) R&G&B (λR,G, B=650 nm, 550 nm, 450 nm). The highest frequency of the input signal is 1 kHz. c) dependence of the input colour channel with the applied voltage

The input wavelength channels are superimposed in the top of the figures to guide the eyes. The reference level was assumed to be the signal when all the input channels were OFF (dark level). In Figure 10a the red frequency was 1.5 KHz and the blue one half of this value while in Figure 10b the ratios between the three frequencies were always one half.

In Figure 10c the dependence of each pulsed single channel with the applied voltage is also displayed. As expected from Figures 5 and 6 the red signal remains constant while the blue and the green decrease as the voltage changes from negative to positive. The lower decrease in the green channel when compared with the blue one is related with to the lower bias dependence of the back diode where a part of the green photons is absorbed.

Data show that the multiplexed signal depends on the applied voltage and on the wavelength and transmission rate of the each input channel. Under reverse bias, there are always four (Figure 28a) or eight (Figure 28b) separate levels depending on the number of input channels. The highest level appears when all the channels are ON and the lowest if they are OFF. Furthermore, the levels ascribed to the mixture of two input channels (R&B, R&G, G&B) are higher than the ones due to the presence of only one (R, G, B). The step among them depends on the applied voltage and channel wavelength. As expected from Figure 22 and Figure 23, as the reverse bias increases the signal exhibits a sharp increase if the blue component is present. Under forward bias the blue signal goes down to zero, so the separated levels are reduced to one half.

In Figure 11a it is displayed the multiplexed signals (solid lines) due to two input channels in the low and high frequency regimes. The transient signals were acquired at different applied voltages (-5V <V<+2V). The blue ($\lambda_L$=450 nm; dotted line) and the red ($\lambda_L$ =650 nm; dash line) input channels are superimposed to guide the eyes across the monochromatic R and B input channels. The red signal frequency was 1.5 KHz and the blue one was half of this value. In Figure 11b the same output signals of Figure 11a are shown, but using for the input frequencies two orders of magnitude lower.

Both figures show that the multiplexed signal depends on the applied voltage and on the frequency regime of the input channels. Results show also that in the high frequency regime (Figure 11a) the multiplexer acts as a charge integrator device while in low frequency regime it works as a differentiator. In the high regime, the output signals (multiplexed signals) show the potentiality of using the device for WDM applications since it integrates every wavelength to a single one retaining the input information.

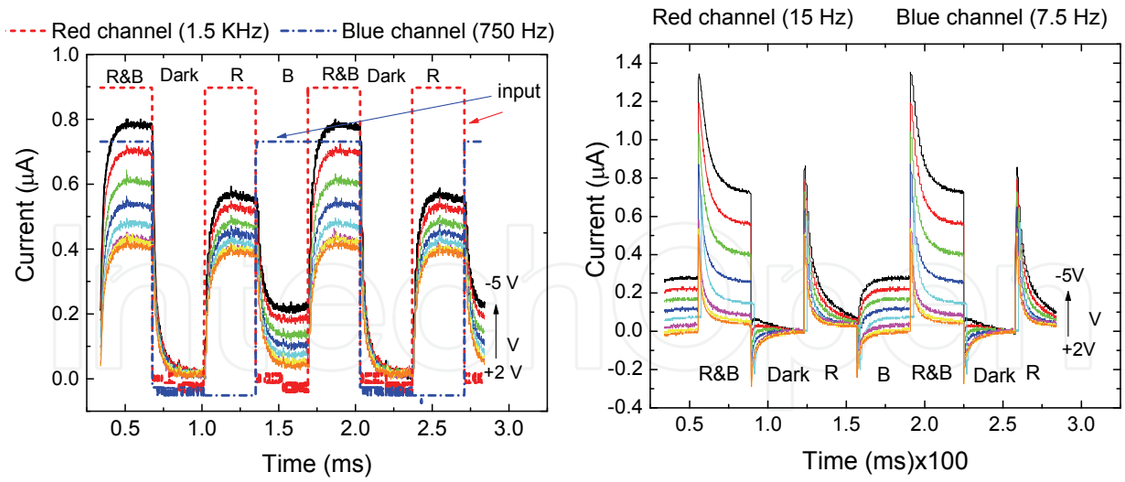


Fig. 11. Wavelength division multiplexing (solid lines) at different applied voltages, obtained using the WDM device: a) High frequency regime. The blue (dotted blue line) and the red (dash-dot red line) guide the eyes into the input channels; b) Low frequency regime.

### 3.2 Bias sensitive multiplexing technique

Figure 12 displays the photocurrent signal obtained with the WDM device under single and combined modulated light bias: red (R: 626 nm), green (G: 524 nm) and blue (B: 470nm) from the glass side. The generated photocurrent is measured under negative (-8V; solid arrow) and positive (+1V, dotted arrow) bias to readout the combined spectra. The light modulation frequency of each channel was chosen to be multiple of the others to ensure a synchronous relation of ON-OFF states along each cycle. For each independent wavelength, the output optical powers were adjusted to give different signal magnitudes at -8V (solid arrows). The correspondent photocurrent signals at +1V are also displayed (dotted arrows). The reference level was assumed when all the input channels were OFF.

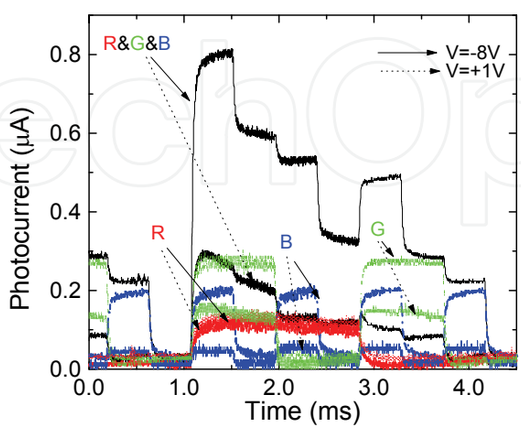


Fig. 12. Multiplexed signals obtained under reverse (solid arrow) and forward (dotted arrow) bias using single (R, G and B) and combined (R&G&B) optical bias of different wavelengths.

As it was expected from Figure 10b, under reverse bias, there are eight separate levels while under positive bias they were reduced to one half. Also, the highest level appears when all the channels are ON and the lowest if they are OFF. Under forward bias the device becomes blind to the front photodiode and the blue component of the combined spectra falls into the dark level, allowing the tuning of the red and green input channels.
In Figure 13 it is shown the multiplexed signals, under reverse and forward bias, obtained with two RGB bit sequences and the same bit rate (2000 bps).

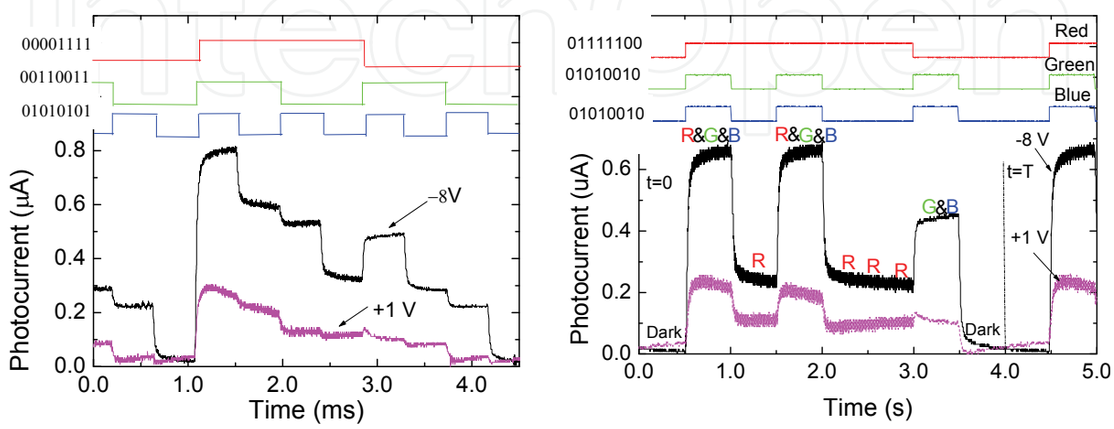


Fig. 13. Multiplexed signals under negative and positive bias using two different bit sequences: a) R [00111100], G [01010010], B[00110011]; b): R [01111100], G [01010010], B[01010010]. On the top, the optical signal used to transmit the information guide the eyes on the different ON-OFF states.

In the bit sequence of Figure 13a (the same of Figure 12) there is a synchronous relation of ON-OFF states along each cycle. The photocurrent under reverse bias, exhibits the expected eight different levels that correspond each to different optical bias states. As the electrical bias goes from reverse to forward the signal amplitude decreases and the levels of the threshold photocurrent associated to each optical state become closer and less defined showing the extinction of the photocurrent caused by the short wavelength optical signals. This mechanism can be used for the identification of the input channels using the photocurrent signal obtained under forward and reverse signals and comparing the magnitude of the variation in each optical state. In the input sequence of Figure 30b the blue and the green channels transmit the same information, and thus the thresholds assigned to the single green or blue channel ON (G or B) and their combination with the red (R&G, R&B) do not appear in the multiplexed signal that contains only four photocurrent levels: R&G&B, G&B, R and Dark.

### 3.3 Influence of the bit rate

In Figure 14 the acquired signals (solid lines) due to the simultaneous presence of two input channels, respectively $\lambda_L$=650 and $\lambda_L$=550 nm, under different values of the modulation light frequencies (1k Hz, 10 kHz and 100 kHz), at –5 V are shown. The superimposed red and green dashed lines correspond to the different input channels, and are displayed just to illustrate the different ON-OFF states of the light bias.

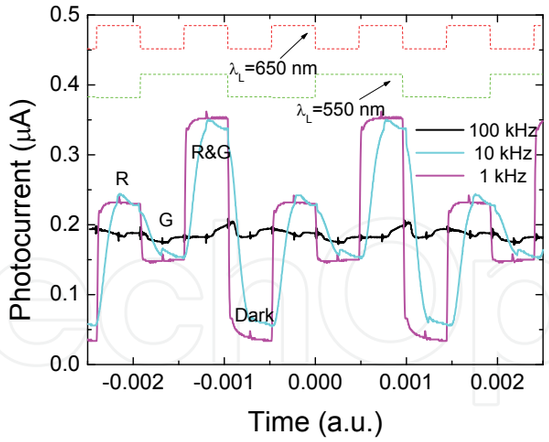


Fig. 14. Wavelength division multiplexing (solid lines) at – 5 V under different values of the modulation light frequency. The red and the green dashed lines guide the eyes into the input channels.

The multiplexed signal shows that in each cycle it is observed for the different frequencies, the presence of the same four levels. The highest occurs when both red and green channels are ON (R&G) and the lower when both are OFF (dark). The green level (G) appears if the red channel is OFF and is lower then the red level (R) that occurs when the green channel is OFF. This behavior is observed even for high frequencies although the measured current magnitude is reduced. So the sensitivity of the device decreases with the increase of the bit rate.

In Figure 15 the multiplexed and the single input channels are shown at different bit rates but with the same bit sequence: a) 2000bps, b) 4000bps. In the top of both figures the bit sequencies are displayed to guide the eyes.

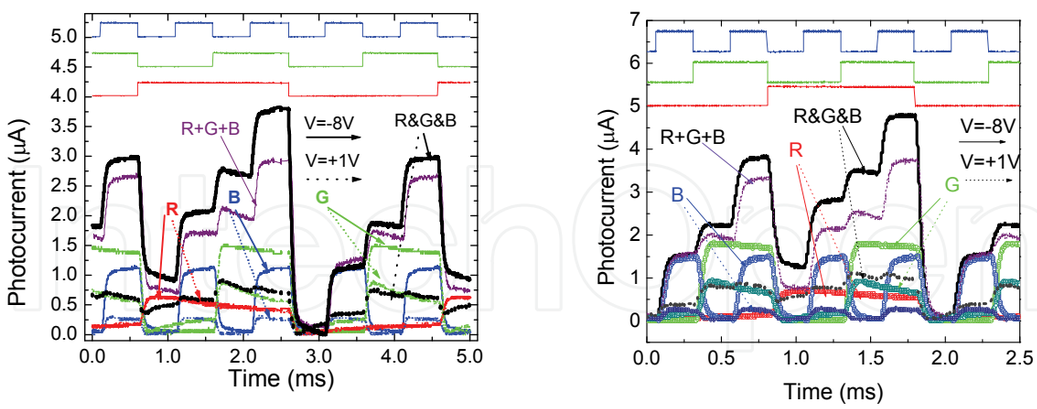


Fig. 15. Multiplexed signals under negative and positive bias using two different bit rates: a) 2000 bps, b) 4000bps. On the top figure, the optical signal used to transmit the information guide the eyes on the different ON-OFF states.

Results show that in the analyzed range, the multiplex signal is independent on the bit rate. It is interesting to notice that in both and under reverse bias, the sum of the input channels is lower than the correspondent multiplexed signals. This optical amplification, mainly on the

ON-ON states, suggests capacitive charging currents due to the time-varying nature of the incident lights.

### 3.4 Influence of optical signal intensity

The identification of the different input channels requires a previous calibration of the transmission signal in order to know the response of the WDM device to each individual channel as the signal attenuation along the transmission medium causes a reduction of the optical intensity at the reception end (WDM device). In order to analyze the influence of this effect the multiplexed signal was acquired with input signals of different optical intensities at -8V and +1V. Measurements were made with different levels of increasing optical power, up to 140 μWcm$^{-2}$.

In Figure 16 it is displayed the output photocurrent density variation with the optical bias measured for each optical channel (R: 626 nm, G: 524 nm and B: 470 nm) at -8 V and + 1V.

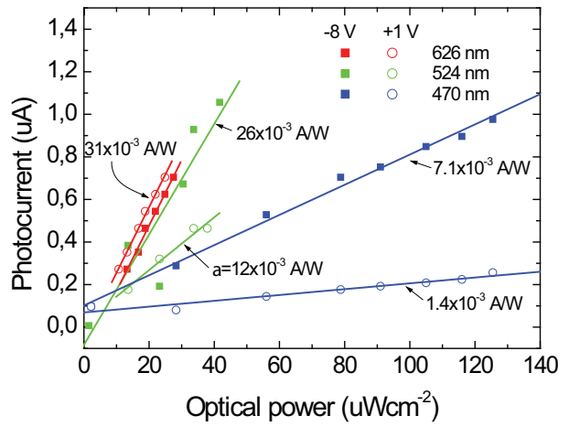


Fig. 16. Photocurrent density variation with the optical bias measured for each optical channel (R: 626 nm, G: 524 nm and B: 470 nm) at -8 V (solid symbols) and + 1V (open symbols). The solid lines correspond to linear fits of the experimental data. Slopes (□) of each plot are also displayed.

Results show that the multiplexed signal magnitude under red illumination and the same intensity conditions is almost independent on the applied bias. Its magnitude increases with the optical power intensity, exhibiting a linear behavior with a growth rate around 31×10$^{-3}$ A/W. Under green and blue light the dependence of the photocurrent magnitude is strongly dependent on the polarity of the applied bias as already demonstrated before. It increases with the optical intensity of each channel either for reverse and forward bias and the growth rate depends on the applied voltage, being higher at reverse bias. Under blue light (470 nm) the growth rate is 5 times higher at reverse than under forward bias, while under green illumination (524 nm) this ratio is only of a factor of 2. This is due to the strong reduction of the device sensitivity for the shorter wavelengths under forward bias.

## 4. Wavelength division demultiplexing device

### 4.1 Bias sensitive wavelength division demultiplexing technique

The major propose of the WDM device is to detect the signal that is being communicated. So, different wavelengths which are jointly transmitted must be separated to regain all the

information. These separators are called demultiplexers. A chromatic time dependent wavelength combination of red and blue or red, green and blue of different transmission rates, were shining on the device. The generated photocurrent was measured under negative and positive bias to readout the combined spectra (Fig. 17).

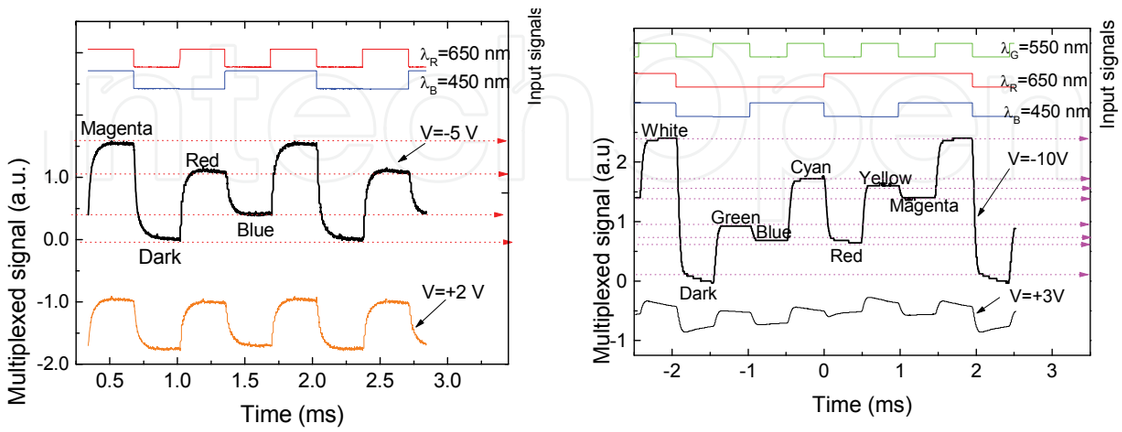


a) b)

Fig. 17. Transient multiplexed signals under negative and positive bias. a) Polychromatic red and blue time dependent mixture. b) Polychromatic red, green and blue time dependent mixture. The digital wavelength demultiplexed signal is displayed on the top of both figures.

If only two R and B channels are involved (four levels; Figure 17a), under forward bias, the blue component of the combined spectra falls into the dark level, tuning the red input channel. Thus, by switching between reverse and forward bias the red and the blue channels were recovered and the transmitted information regained. If three R, G and B input channels with different transmission rates are being used (eight levels, Figure 17b), under reverse bias, the levels can be grouped into four main thresholds, ascribed respectively to the simultaneous overlap of three (R&G&B), two (R&B, R&G, B&G), one (R, G, B) and none (dark) input channels. Since under forward bias, the blue component of the multiplexed signal approaches the dark level the R, the G and the R&G components are tuned. By comparing the multiplexed signals under forward and reverse bias and using a simple algorithm that takes into account the different sub-level behaviors under reverse and forward bias (Figure 17b) it is possible to split the red from the green component and to decode their RGB transmitted information. The digital wavelength division demultiplex signals are displayed on the top of both figures.

In Figure 18, it is displayed the photocurrent generated by the combination of two red and blue input channels in short circuit (open symbol) and under reverse bias (line). Results show that under short circuit the blue component of the combined spectra falls into the dark level, tuning the red input channel. Thus, by switching between short circuit and reverse bias the red and the blue channels were recovered.

The device acts as a charge integrator, keeping the memory of the input channel. So, it can be used as a non selective division wavelength multiplexing device, WDM.

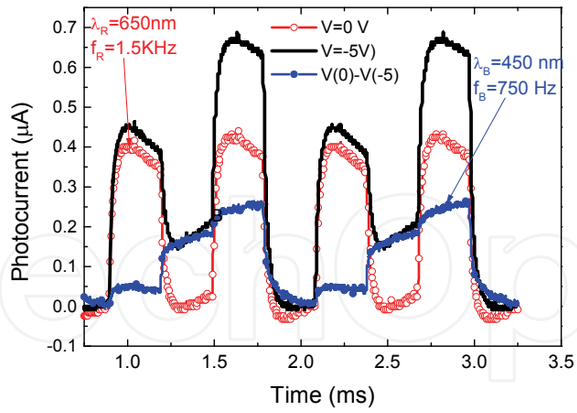


Fig. 18. Blue and red wavelength division demultiplexing output channels (dot lines) for the input signal (solid line).

### 4.2 Signal recovery

In Figure 19 it is displayed, under reverse and forward bias, the multiplexed signals due to the simultaneous transmission of three independent bit sequences, each one assigned to one of the RGB color channels. On the top, the optical signal used to transmit the information is displayed to guide the eyes on the different ON-OFF states. The bit sequence obtained for the demultiplexed signal is also shown for comparison.

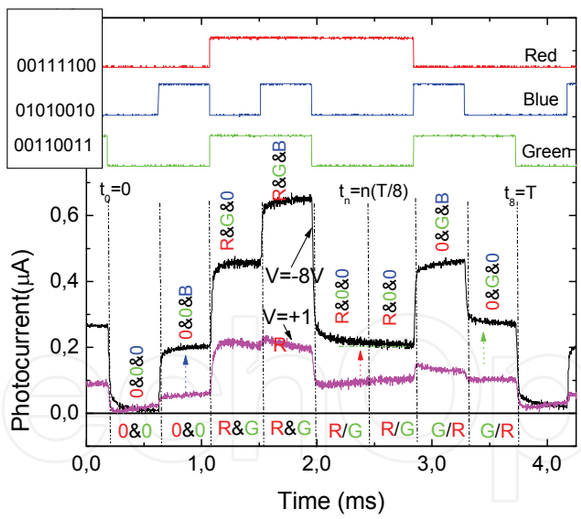


Fig. 19. Multiplexed signals under reverse and forward bias. On the top, the optical signal used to transmit the information guide the eyes on the different ON-OFF states. The bit sequence for the demultiplexed signal is shown for comparison.

To recover the transmitted information (8 bit per wavelength channel) the multiplexed signal, during a complete cycle (0<t<T), was divided into eight time slots, each corresponding to one bit where the independent optical signals can be ON (1) or OFF (0). As, under forward bias, the WDM device has no sensitivity to the blue channel, the red and green transmitted information can be identified from the multiplexed signal at +1V. The

highest level corresponds to both channels ON (R&G: R=1, G=1), and the lowest to the OFF-OFF stage (R=0; G=0). The two levels in-between are related with the presence of only one channel ON, the red (R=1, G=0) or the green (R=0, G=1) (see horizontal labels in Figure 19). To distinguish between these two situations and to decode the blue channel, the correspondent sub-levels, under reverse bias, have to be analyzed. From Figure 10, 12 and 15 it is observed that the green channel is more sensitive to changes on the applied voltage than the red, and that the blue only appears under reverse bias. So, the highest increase at -8V corresponds to the blue channel ON (B=1), the lowest to the ON stage of the red channel (R=1) and the intermediate one to the ON stage of the green (G=1) (see colour arrows and vertical labels in Figure 36). Using this simple algorithm the independent red, green and blue bit sequences can be decoded as: R[00111100], G[00110011] and B[01010010].

To validate the ability of this device to multiplex and demultiplex optical signals, the multiplexed signals, in Figure 12, were analysed, in a time window between 0.7ms and 4.2ms, resulting in the bit sequences: R[11110000], G[11001100] and B[10101010] which are in agreement with the signals acquired for the independent channels.

A demux algorithm was implemented in Matlab that receives as input the measured photocurrent and derives the sequence of bits that originated it. The algorithm makes use of the variation of the photocurrent instead of its absolute intensity to minimise errors caused by signal attenuation. A single linkage clustering method is applied to find automatically eight different clusters based on the measured current levels in both forward and reverse bias. This calibration procedure is performed for a short calibration sequence. Each cluster is naturally bound to correspond to one of the known eight possible combinations of red, green and blue bits. Following this procedure the sequence of transmitted bits can be recovered in real time by sampling the photocurrent at the selected bit rate and finding for each sample the cluster with closest current levels. In Figure 20 we present an example of the output obtained for two different sequences at 4000 bps.

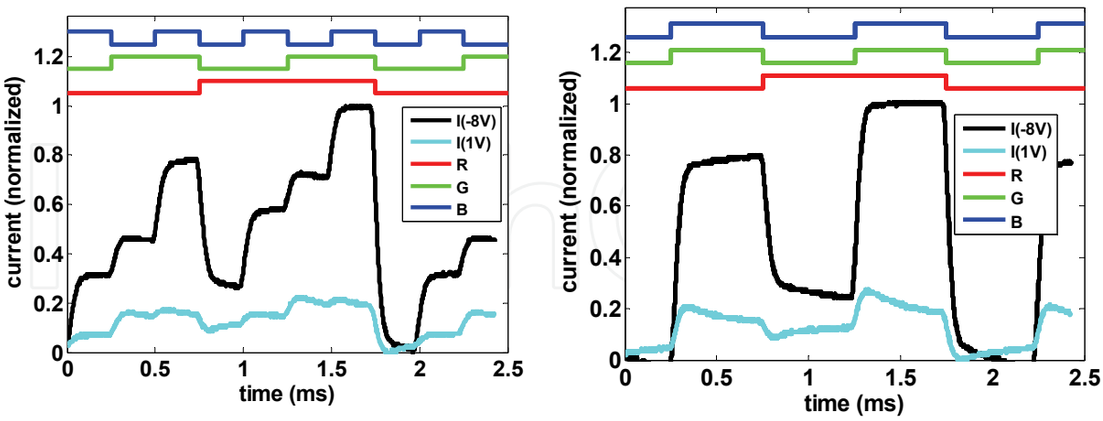


Fig. 20. A snapshot of the output from the MatLab routine used to demux the transmitted sequence of bits. The sequence of red, green and blue bits (shown at the top) was derived from the measured currents.

Output data of the demux algorithm show that the derived sequences are R [00011100], G [011001100] and B [10101010] for the multiplexed signal of Figure 20a and R [00011100], G

[011001100] and B [011001100] for Figure 20b. Both were found to be in exact agreement with the original sequences of bits that were transmitted. These observations indicate that it is possible to improve the performance of the WDM device without adding any optical pre-amplifier or optical filter, which is an advantage when compared with the standard p-i-n cells. The impulsive response of the nano-optical filter is bias controlled and the recovery algorithm is very simple, without the limiting factors associated with the operation of an optical complex receiver structure when using a standard p-i-n cell.

## 5. Signal attenuation

The identification of the different input channels requires a previous calibration of the transmission signal in order to know the response of the WDM device to each individual channel as the signal attenuation along the transmission medium causes a reduction of the optical intensity at the reception end (WDM device). In order to analyze the influence of this effect the multiplexed signal was acquired with input signals of different optical intensities.
In Figure 21 the output multiplexed signal is displayed at -8V and +1V for different optical power intensities of the different input channels. Measurements were made with three levels of increasing optical power, starting with R= 11 μWcm$^{-2}$; G= 14 μWcm$^{-2}$; B= 28 μWcm$^{-2}$ (I=1×) and then for twice (I=2×: R = 13 μWcm$^{-2}$; G = 28 μWcm$^{-2}$;B = 56 μWcm$^{-2}$) and five times (I=5×: R= 22 μWcm$^{-2}$; G= 38 μWcm$^{-2}$;B = 105 μWcm$^{-2}$) more current to drive the LEDs.

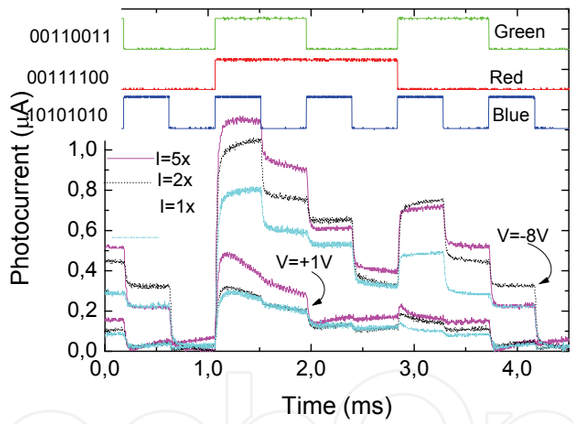


Fig. 21. Multiplexed signal at -8V and +1V under different optical power intensities of the RGB input channels.

Results show that under reverse bias, as the channel intensity decreases, the multiplexed output signal also decreases. Under forward bias the signal is almost unaltered for the lowest intensities.

## 6. Linearity

In Figure 22 it is displayed the multiplexed signal obtained at reverse bias, under monochromatic light bias of different wavelengths ($\lambda_R$=650 nm, $\lambda_G$=550 nm, $\lambda_B$=450 nm) and dual wavelengths combinations ($\lambda_R$=650 nm & $\lambda_G$=550 nm and $\lambda_R$=650 nm & $\lambda_B$=450 nm). The light modulation frequency of one the light bias was chosen to be half of the other in order to ensure a synchronous relation of ON-OFF states along each cycle.

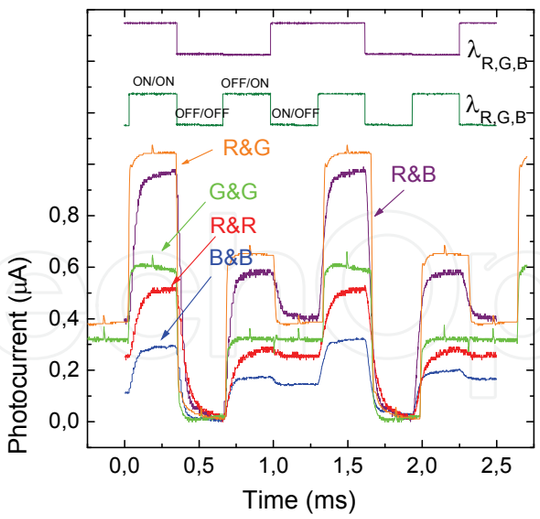


Fig. 22. Multiplexed signals at – 5V and under different input light bias: R&R ($\lambda_{R,R}$=650,650 nm); G&G($\lambda_{G,G}$=550,550 nm), B&B ($\lambda_{B,B}$= 450,450 nm), R&B($\lambda_{R,B}$=650,450 nm) and R&G($\lambda_{R,G}$=650,550 nm).

Under monochromatic illumination the ON-ON state corresponds to the maximum intensity of light bias, while the ON-OFF and OFF-ON to a lower intensity and the OFF-OFF to the dark conditions. Results suggest that for every wavelength the photocurrent signal exhibits linearity, as its magnitude is maximum in the ON-ON state, lower and constant in both OFF-ON and ON-OFF states (half of the observed in the ON-ON state) and minimum in the OFF-OFF state. The highest photocurrent signal under monochromatic illumination is obtained with green light ($\lambda_G$=550 nm), followed by the red ($\lambda_R$=650 nm) and then by the blue ($\lambda_B$=450 nm). The multiplexed signal obtained under red and green bias ($\lambda_R$=650 nm & $\lambda_G$=550 nm) or red and blue bias ($\lambda_R$=650 nm & $\lambda_B$=450 nm) shows four different magnitude levels of photocurrent corresponding each to the conditions of states of the light bias.

## 7. Self optical amplification

### 7.1 Self bias amplification under transient conditions and uniform irradiation

When an external electrical bias (positive or negative) is applied to a double pin structure, its main influence is in the field distribution within the less photo excited sub-cell [M. Vieira et al 2008]. The front cell under red irradiation, the back cell under blue light and both under green steady state illumination. In comparison with thermodynamic equilibrium conditions (dark), the electric field under illumination is lowered in the most absorbing cell (self forward bias effect) while the less absorbing reacts by assuming a reverse bias configuration (self reverse bias effect).

In Figure 23, the spectral photocurrent at different applied voltages is displayed under red (a), green (b) and blue (c) background irradiations and without it (d).

Results confirm that a self biasing effect occurs under unbalanced photogeneration. As the applied voltages changes from positive to negative the blue background enhances the spectral sensitivity in the long wavelength range. The red bias has an opposite behavior since the spectral sensitivity is only increased in the short wavelength range. Under green background the spectral photocurrent increases with the applied voltage everywhere.

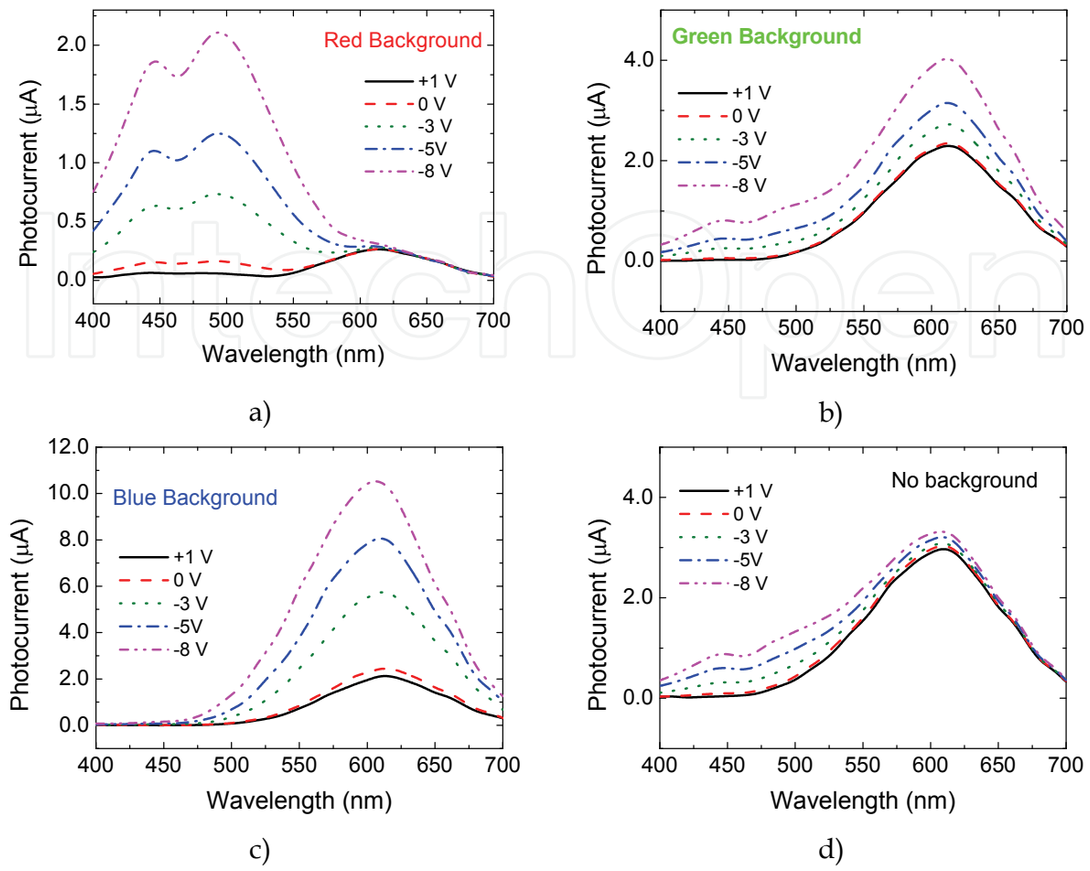


Fig. 23. Spectral photocurrent under reverse and forward bias measured without and with ($\lambda_L$) background illumination.

As expected, results show that the blue background enhances the light-to-dark sensitivity in the long wavelength range and quenches it in the short wavelength range. The red bias has an opposite behavior; it reduces the ratio in the red/green wavelength range and amplifies it in the blue one.

In Figure 24 the spectral is displayed at negative and positive electrical bias; without and under red (626 nm), green (524 nm) and blue (470 nm;) background illumination from the p side.

We have demonstrated that when an external electrical bias is applied to a double pin structure, its major influence is in the field distribution within the less photo excited sub-cell. The front cell when under red irradiation, the back cell when under blue light and both when under green steady state illumination. In comparison with thermodynamic equilibrium (no background), the electric field under illumination is lowered in the most absorbing cell (self forward bias effect) while in the less absorbing cell reacts by assuming a reverse bias configuration (self reverse bias effect).

Results confirm that, under negative bias, a self biasing effect occurs under an unbalanced photogeneration. Blue optical bias enhances the spectral sensitivity in the long wavelength ranges and quenches it in the short wavelength range. The red bias has an opposite behavior: it reduces the collection in red/green wavelength ranges and amplifies in the blue

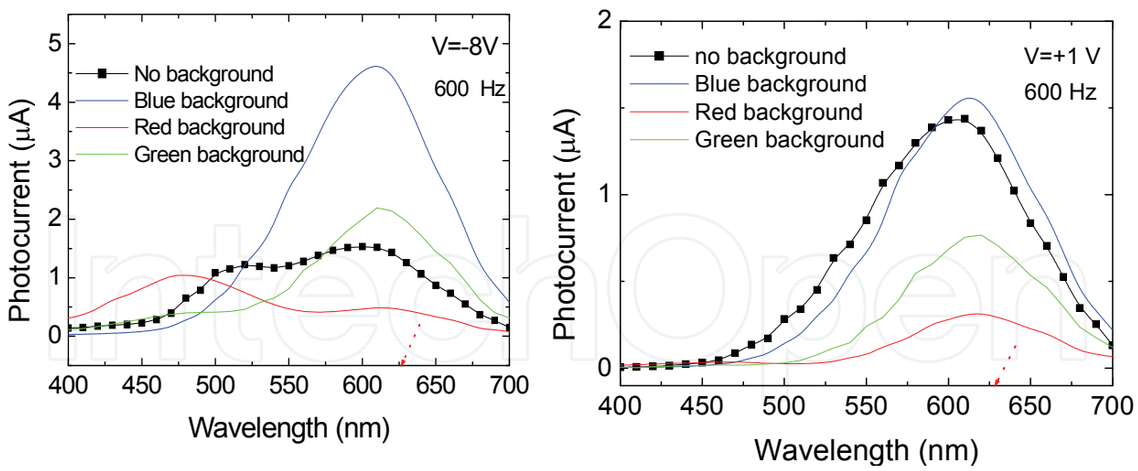


Fig. 24. Spectral photocurrent @ +1 V, -8 V without (dark) and under red, green and blue optical bias.

range. The green optical bias only reduces the spectral photocurrent in the medium wavelength range keeping the other two almost unchangeable. Under positive bias no significant self bias effect was detected. This voltage controlled light bias dependence gives the sensor its light-to-dark sensitivity allowing the recognition of a color image projected on it. In Figure 25 the ratio between the spectral photocurrents under red, green and blue steady state illumination and without it (dark) is plotted.

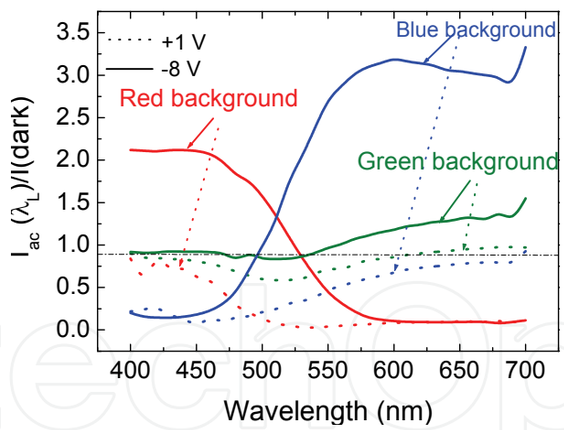


Fig. 25. Ratio between the photocurrents under red, green and blue steady state illumination and without it (dark).

The sensor is a wavelength current-controlled device that makes use of changes in the wavelength of the optical bias to control the power delivered to a load, acting as an optical amplifier. Its gain, defined as the ratio between the photocurrent with and without a specific background depends on the background wavelength that controls the electrical field profile across the device. If the electrical field increases locally (self optical amplification) the collection is enhanced and the gain is higher than one. If the field is reduced (self optical quench) the collection is reduced and the gain is lower than one. This optical nonlinearity makes the transducer attractive for optical communications.

### 7.2 Optical bias controlled wavelength discrimination

Figure 26 shows the time dependent photocurrent signal measured under reverse (-8V, symbols) and forward (+1V, dotted lines) bias using different input optical signals without (no bias) and with ($\lambda_L$) red, green and blue steady state additional optical bias. Both optical signals and steady state bias were directed onto the device by the side of the a-SiC:H thin structure. The optical signals were obtained by wave square modulation of the LED driving

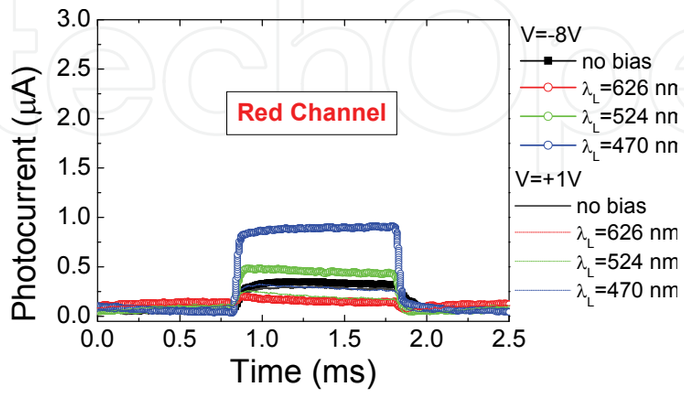


a)

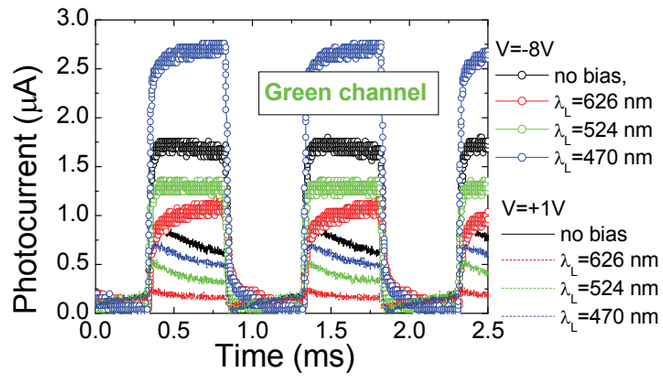


b)

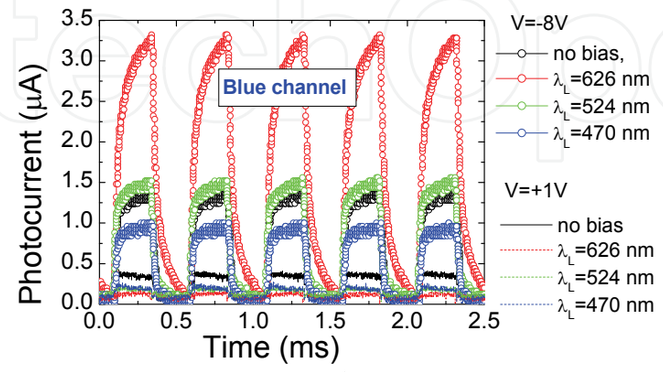


c)

Fig. 26. Red (a), green (b) and blue (b) channels under reverse and forward voltages without and with ($\lambda_L$) red, green and blue steady state bias.

current and the optical power intensity of the red, green and blue channels adjusted to 51, 90, 150 μW/cm², respectively. The steady state light was brought in LEDS driven at a constant current value (R: 290 μW/cm², G: 150 μW/cm², B: 390 μW/cm²).
Results show that the blue steady state optical bias amplifies the signals carried out by the red (Figure 26a) and the green channels (Figure 26b) and reduces the signal of the blue channel (Figure 26c). Red steady state optical bias has an opposite behavior, reinforcing the blue channel and decreasing the blue and the green channels. The green optical bias mainly affects the green channel, as the output signal is reduced while the signals of the red and blue channels show negligible changes.
When an optical bias is applied, it mainly enhances the field distribution within the less photo excited sub-cell: the back under blue irradiation and the front under red steady bias. Therefore, the reinforcement of the electric field under blue irradiation and negative bias increases the collection of carriers generated by the red channel and decreases the blue one. Under red optical bias, the opposite behavior is observed. The green bias absorption is balanced in both front and back cells and the collection of carriers generated by the green channel is strongly reduced. This optical nonlinearity makes the transducer attractive in optical communications. This nonlinear effect, under transient conditions, is used to distinguish a wavelength, to read a color image, to amplify or to suppress a color channel add and drop an optical signal.
In Figure 27, for the same bit sequence of Figure 19, the multiplexed signal is displayed.

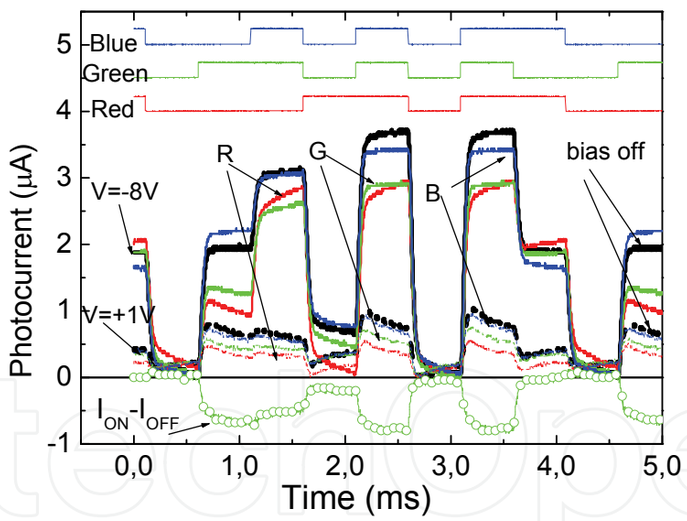


Fig. 27. Multiplexed signals at -8V/+1V (solid /dot lines); without (bias off) and with (R, G, B) optical bias.

Results confirm that under appropriated homogeneous wavelength irradiation it is possible to select or to suppress a color channel without having to demultiplex the stream.

### 7.2 Self bias amplification under transient conditions and uniform irradiation

A chromatic time dependent wavelength combination (4000 bps) of R ($\lambda_R$=624 nm), G ($\lambda_G$=526 nm) and B ($\lambda_B$=470 nm) pulsed input channels with different bit sequences, was used to generate a multiplexed signal in the device. The output photocurrents, under

positive (dot arrows) and negative (solid arrows) voltages with (colour lines) and without (dark lines) background are displayed in Figure 28. The bit sequences are shown at the top of the figure.

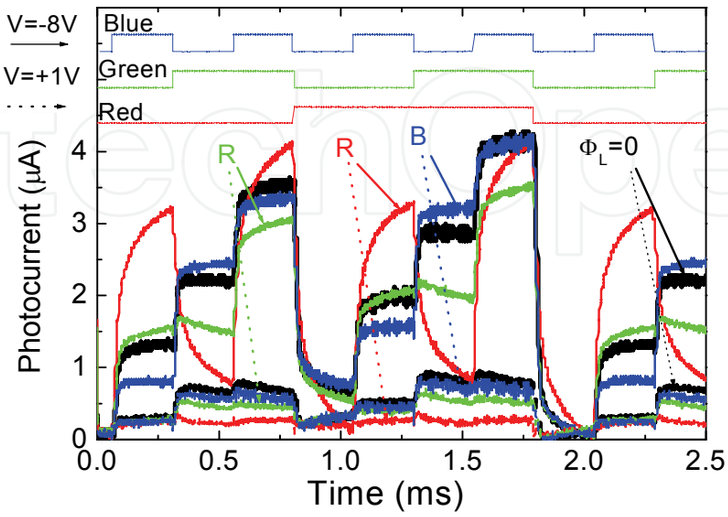


Fig. 28. Single and combined signals at -8V; without (solid arrows) and with (dotted arrows) red, green and blue optical bias.

Results show that, even under transient input signals (the input channels), the background wavelength controls the output signal. This nonlinearity, due to the transient asymmetrical light penetration of the input channels across the device together with the modification on the electrical field profile due to the optical bias, allows tuning an input channel without demultiplexing the stream.

## 8. Conclusions

In this chapter we present results on the optimization of multilayered a-SiC:H heterostructures for wavelength-division (de) multiplexing voltage control.

The non selective WDM device is a double heterostructure in a glass/ITO/a-SiC:H (p-i-n) /a-SiC:H(-p) /a-Si:H(-i?)/a-SiC:H (-n?)/ITO configuration. The single or the multiple modulated wavelength channels are passed through the device, and absorbed accordingly to its wavelength, giving rise to a time dependent wavelength electrical field modulation across it. The effect of single or multiple input signals is converted to an electrical signal to regain the information (wavelength, intensity and frequency) of the incoming carriers. Here, the (de) multiplexing channels is accomplished electronically, not optically. This approach has advantages in terms of cost since several channels share the same optical components; and the electrical components are typically less expensive than optical ones. An electrical model gives insight into the device operation.

Stacked structures that can be used as wavelength selective devices, in the visible range, are analysed. Two terminal heterojunctions ranging from p-ií-n to p-i-n-p-i'-n configurations are studied. Three terminals double staked junctions with transparent contacts in-between are also considered to increase wavelength discrimination. The color discrimination was achieved by ac photocurrent measurement under different externally applied bias.

Experimental data on spectral response analysis and current –voltage characteristics are reported. A theoretical analysis and an electrical simulation procedure are performed to support the wavelength selective behavior. Good agreement between experimental and simulated data was achieved. Results show that in the single p-i-n configuration the device acts mainly as an optical switch while in the double ones, due to the self bias effect, the input channels are selectively tuned by shifting between positive and negative bias. If the internal terminal is used the inter-wavelength cross talk is reduced and the S/N increased.
Results show that by switching between positive and negative voltages the input channels can be recovered or removed. So, this optical device allows to add and drop one or several channels in a WDM optical network (OADMS) and can be used in optical communications.
Three modulated input channels were transmitted together, each one located at different wavelength and frequencies. The combined optical signal was analyzed by reading out the photocurrent generated across the device.
A physical model supported by an electrical and a numerical simulation gives insight into the device operation. Voltage controlled multiplexing devices, in multilayered a-SiC:H pin architectures, were compared.
Experimental and simulated results show that the device acts as a charge transfer system. It filters, stores and transports the minority carriers generated by current pulses, keeping the memory of the input channels (color and transmission speed). In the stacked configuration, both front and back transistors act separately as wavelength selective devices, and are turned on and off sequentially by applying current pulses with speed transmissions dependent off the on-off state of all the input channels.
To enhance the bandwidth of the optical transmission system more work has to be done in order to enlarge the number of input channels and to improve the frequency response.

## 9. References

A. Fantoni, M. Vieira, R. Martins, Mathematics and Computers in Simulation, Vol. 49. (1999) 381-401.

A. Zhu, S. Coors, B. Schneider, P. Rieve, M. Bohm, IEEE Trans. on Electron Devices, Vol. 45, No. 7, July 1998, pp. 1393-1398.

D. Nolan K. O. Hill et all, Fiber Optics HandbookFiber, Devices, and Systems for Optical Communications McGraw Hill 2002

G. de Cesare, F. Irrera, F. Lemmi, F. Palma, IEEE Trans. on Electron Devices, Vol. 42, No. 5, May 1995, pp. 835-840.

H. Stiebig, J. Gield, D. Knipp, P. Rieve, M. Bohm, Mat. Res. Soc. Symp. Proc 337 (1995) 815-821.

H.K. Tsai, S.C. Lee, IEEE electron device letters, EDL-8, (1987) pp.365-367. .

M. Bas, Fiber Optics Handbook, Fiber, Devices and Systems for Optical Communication, Chap, 13, Mc Graw-Hill, Inc. 2002.

M. G. Kuzyk, Polimer Fiber Optics, Materials Physics and Applications, Taylor and Francis Group, LLC; 2007.

M. Haupt, C. Reinboth and U. H. P. Fischer. "Realization of an Economical Polymer Optical Fiber Demultiplexer", Photonics and Microsystems, 2006 International Students and Young Scientists Workshop, Wroclaw, 2006.

M. Kagami. "Optical Technologies for Car Applications Innovation of the optical waveguide device fabrication". Optical communications - perspectives on next generation technologies, October 23-25, 2007 in Tokyo, Japan.

M. Mulato, F. Lemmi, J. Ho, R. Lau, J. P. Lu, R. A. Street, J. of Appl. Phys., Vol. 90, No. 3 (2001), pp. 1589-1599.

M. Topic, H. Stiebig, D. Knipp, F. Smole, J. Furlan, H. Wagner, J. Non Cryst. Solids 266-269 (2000) 1178-1182.

M. Vieira, A. Fantoni, M. Fernandes, P. Louro, G. Lavareda and C.N. Carvalho, Thin Solid Films, 515, Issue 19, 2007, 7566-7570.

M. Vieira, A. Fantoni, P. Louro, M. Fernandes, R. Schwarz, G. Lavareda, and C. N. Carvalho, Vacuum, Vol. 82, Issue 12, 8 August 2008, pp: 1512-1516.

M. Vieira, A. Fantoni, P. Louro, M. Fernandes, R. Schwarz, G. Lavareda, C.N. Carvalho "Self-biasing effect in colour sensitive photodiodes based on double p-i-n a-SiC:H heterojunctions" Vacuum, Volume 82, Issue 12, 8 August 2008, pp 1512-1516.

M. Vieira, M. Fernandes, A. Fantoni, P. Louro, M. A. Vieira, "Large area a-SiC:H WDM devices for signal multiplexing and demultiplexing in the visible spectrum", Thin Solid Films, (In Press).

M. Vieira, M. Fernandes, J. Martins, P. Louro, R. Schwarz, and M. Schubert, IEEE Sensor Journal, 1, 2001, 158-167.

M. Vieira, M. Fernandes, P. Louro, A. Fantoni, M. Barata, M A Vieira, "Multilayered a-SiC:H device for Wavelength-Division (de)Multiplexing applications in the visible spectrum" Symposium A: S. Francisco, USA, 24 -29 March, 2008, in Amorphous and Polycrystalline Thin-Film Silicon Science and Technology, edited by A. Flewitt, J. Hou, S. Miyazaki, A. Nathan, and J. Yang (Mater. Res. Soc. Symp. Proc. Volume 1066, Warrendale, PA, 2008), pp.225-230 A08-01.

O. Ziemann, J. Krauser, P.E. Zamzow, W. Daum, POF Handbook, Optical Short Range Transmission Systems, Springer, 2nd Ed., 2008.

P. Louro, M. Vieira, M A Vieira, M. Fernandes, A. Fantoni, C. Francisco, M. Barata "Optical multiplexer for short range application" Physica E: Low-dimentional Systems and Nanostructures , In Press, Corrected Prof, Available online20, August 2008

P. Louro, M. Vieira, Yu. Vygranenko, A. Fantoni, M. Fernandes, G. Lavareda, N. Carvalho Mat. Res. Soc. Symp. Proc., 989 (2007) A12.04.

P. Louro, Y. Vygranenko, J. Martins, M. Fernandes and M. Vieira "Colour sensitive devices based on double p-i-n-i-p stacked photodiodes" Thin Solid Films Vol. 515, Issue 19, 16 July 2007, pp 7526-7529.

S. Randel, A.M.J. Koonen, S.C.J. Lee, F. Breyer, M. Garcia Larrode, J. Yang, A. Ng'Oma, G.J Rijckenberg, H.P.A. Boom. "Advanced modulation techniques for polymer optical fiber transmission". proc. ECOC 07 (Th 4.1.4). Berlin, Germany (2007) 1-4.

W. Daum, J. Krauser, P.E. Zamzow, O.Ziemann."Polimer Optical Fibers for Data Communication" Springer-Verlag, 2002.

W. Stallings, "Data and Computer Communications", Pearson Education, Inc., 2007. p.247-248

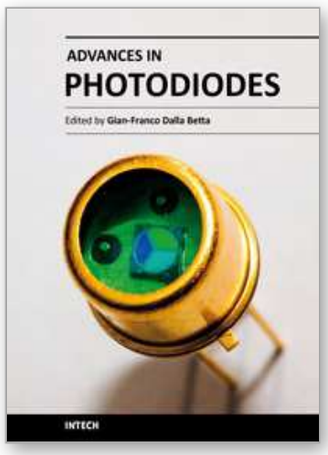


**Advances in Photodiodes**

Edited by Prof. Gian Franco Dalla Betta

ISBN 978-953-307-163-3
Hard cover, 466 pages
**Publisher** InTech
**Published online** 22, March, 2011
**Published in print edition** March, 2011

Photodiodes, the simplest but most versatile optoelectronic devices, are currently used in a variety of applications, including vision systems, optical interconnects, optical storage systems, photometry, particle physics, medical imaging, etc. Advances in Photodiodes addresses the state-of-the-art, latest developments and new trends in the field, covering theoretical aspects, design and simulation issues, processing techniques, experimental results, and applications. Written by internationally renowned experts, with contributions from universities, research institutes and industries, the book is a valuable reference tool for students, scientists, engineers, and researchers.

**How to reference**

In order to correctly reference this scholarly work, feel free to copy and paste the following:

P. Louro, M. Vieira, M. A. Vieira, M. Fernandes and J. Costa (2011). Use of a-SiC:H Photodiodes in Optical Communications Applications, Advances in Photodiodes, Prof. Gian Franco Dalla Betta (Ed.), ISBN: 978-953-307-163-3, InTech, Available from: http://www.intechopen.com/books/advances-in-photodiodes/use-of-a-sic-h-photodiodes-in-optical-communications-applications

INTECH
open science | open minds

**InTech Europe**
University Campus STeP Ri
Slavka Krautzeka 83/A
51000 Rijeka, Croatia
Phone: +385 (51) 770 447
Fax: +385 (51) 686 166
www.intechopen.com

**InTech China**
Unit 405, Office Block, Hotel Equatorial Shanghai
No.65, Yan An Road (West), Shanghai, 200040, China
中国上海市延安西路65号上海国际贵都大饭店办公楼405单元
Phone: +86-21-62489820
Fax: +86-21-62489821

IntechOpen